Tropical coral reef habitat in a geoengineered, high-CO_2 world

Authors: E. Couce [1,2], P.J. Irvine [3], L. J. Gregorie [2], A. Ridgwell [2], E.J. Hendy [1,4]*

[1] *School of Earth Sciences, Queens Road, University of Bristol, Bristol BS8 1RJ, UK*

[2] *School of Geographical Sciences, University of Bristol, Bristol BS8 1SS, UK*

[3] *Institute for Advanced Sustainability Studies, 130 Berliner Strasse, Potsdam 14467, Germany*

[4] *School of Biological Sciences, Woodland Road, University of Bristol, Bristol BS8 1UG, UK*

*Corresponding author: e.hendy@bristol.ac.uk, Tel: +44 (0)117-331-5003

Key points:

• Large reductions in reef habitat suitability under net radiative >3 W/m^2.

• Rising SSTs are greater threat for tropical coral reefs than ocean acidification.

• Solar Radiation Management may help maintain coral reef habitat over near-term.

Abstract

Continued anthropogenic CO_2 emissions are expected to impact tropical coral reefs by further raising sea surface temperatures (SST) and intensifying ocean acidification (OA). Although geoengineering by means of Solar Radiation Management (SRM) may mitigate temperature increases, OA will persist, raising important questions regarding the impact of different stressor combinations. We apply statistical Bioclimatic Envelope Models to project changes in shallow-water tropical coral reef habitat as a single niche (without resolving biodiversity or community composition) under various Representative Concentration Pathway and SRM scenarios, until 2070. We predict substantial reductions in habitat suitability centered on the Indo-Pacific Warm Pool under net anthropogenic radiative forcing of ≥3.0 W/m^2. The near-term dominant risk to coral reefs is increasing SSTs; below 3 W/m^2 reasonably favorable conditions are maintained, even when achieved by SRM with persisting OA. 'Optimal' mitigation occurs at 1.5 W/m^2 because tropical SSTs over-cool in a fully-geoengineered (i.e. pre-industrial global mean temperature) world.

Index terms:

1622, 1630, 4220, 1635, 1615

1. Introduction

Tropical shallow-water coral reefs cover 0.1% of the World's oceans, yet rank amongst the most productive and biodiverse ecosystems. Anthropogenic pressures have been implicated in significant long-term reef decline, as well as abrupt coral mortality events associated with extreme temperatures and bleaching [*Hoegh-Guldberg et al.* 2007]. Solar Radiation Management (SRM) –a form of geoengineering achieved by adding reflective aerosols to the atmosphere [*Crutzen*, 2006], increasing cloud albedo [*Latham and Smith*, 1990], or increasing the albedo of the Earth's surface [*Irvine et al.*, 2011], for example– has the potential to mitigate surface warming and hence hypothetically help safe-guard shallow-water coral reef habitat. But by only seeking to diminish downward radiation [*Angel*, 2006], SRM achieves no direct mitigation of atmospheric CO_2 and resulting 'ocean acidification'. The latter undermines habitat construction that supports coral reef ecosystems because higher pCO_2 reduces carbonate ion concentration and associated saturation (Ω_{Arag}) levels, in turn lowering net carbonate production by corals and calcareous algae [*Kleypas et al.*, 1999].

Any implementation of SRM geoengineering would, therefore, produce a complex pattern of marine environmental changes, overall characterized by relatively low sea surface temperatures (SST) but with high levels of atmospheric pCO_2 and ocean acidification. This raises important questions about the primary global environmental threat(s) to tropical coral reefs: whether it is increased SSTs, reduced Ω_{Arag}, or that both factors are equally significant. Our motivation in this paper is hence not to make a case for or against SRM, but to explore the spatial and temporal consequences of different potential global temperature and ocean acidification futures for shallow-water coral reefs. Bioclimatic Envelope Modeling can be applied to forecast effects of climate change on species' distribution [e.g. *Thuiller et al.* 2005] and statistically analyze the environmental requirements of coral reef ecosystems [*Couce et al.*, 2012]. We use this approach to explore how changing future environmental conditions with and without SRM geoengineering could affect the potential suitability of global shallow water habitats for coral reef ecosystems.

2. Methods

Bioclimatic Envelope Modeling analyzes the relationship between environmental factors and the distribution of a species (or an ecosystem), using statistical correlation to identify acceptable environmental ranges and the relative significance of the different factors. We used two machine-learning techniques: Maximum Entropy [MaxEnt; *Phillips et al.*, 2006] and Boosted Regression Trees [BRT; *Friedman*, 2001]. The assumption behind MaxEnt is that a species/ecosystem will occupy all suitable habitat in as random a way as possible; MaxEnt then identifies which constraints maximize the entropy of the system. BRT is based on decision trees. A single tree is built by repeatedly finding a simple rule (whether one of the predictive variables is above or below a specific threshold) that can split the data into groups providing the best separation of presence and absence sites. A sequence of trees (typically >1000) is produced, each grown on reweighted versions of the data, with final predictions obtained from the weighted average across the tree sequence.

Couce *et al.* [2012] provides a detailed analysis and background to BRT and MaxEnt in relation to establishing environmental controls on tropical coral reef biogeography. In the current study 12 environmental fields were considered including SST, Ω_{Arag}, salinity, nutrients, and light availability. We chose Ω_{Arag} over pH because coral calcification is directly linked to saturation state, although under rapid fossil fuel CO_2 release changes in both variables will be closely correlated [*Hönisch et al.*, 2012]. In total 27 predictive variables were used by including mean annual and extreme monthly values for most fields, in addition to weekly extremes and standard deviation of SST (for complete list and relative contribution to predictions see Appendix S1). All model training datasets were based on observations except Ω_{Arag} and SST, which were obtained from 1990 projections of the University of Victoria (UVic) Earth System Climate Model [*Weaver et al.*, 2001; *Turley et al.*, 2010] of open ocean water in proximity to reefs. All fields were mapped onto a 1°x1° global grid between 60°S and 60°N; for cells outside the open-ocean mask environmental data was extrapolated up to 1° by linear average of neighboring cells. The models were trained on a "shallow water mask" defined by bathymetry within the euphotic zone and the area covered by UVic projections (Fig. S1.1). Locations of shallow-water reef and coral communities were taken from Reefbase [version 2000] and projected on the 1°x1° grid as binary presence/absence data. See Appendix S1 and *Couce et al*. [2012] for further details on model development and variables.

Future and pre-industrial (P-I) projections of mean annual SST and Ω_{Arag} were determined using the UVic model [*Weaver et al.*, 2001] version 2.9, which comprises an atmosphere Energy Moisture Balance Model coupled to a 3D ocean general circulation model, both at a spatial resolution of 1.8° x 3.6°. Ocean chemistry was calculated by the biogeochemical and carbon cycle model of Schmittner *et al*. [2008]. The UVic model was forced with concentrations of CO_2 and other greenhouse gases from the Representative Concentration Pathways [RCPs; *Moss et al.*, 2010] developed for the 5th Assessment Report of the Intergovernmental Panel on Climate Change corresponding to a total anthropogenic radiative forcing of 3, 4.5, 6 and 8.5 W/m^2 above P-I at 2100 respectively (labeled 'RCP 3' to 'RCP 8.5'). The extent of SRM geoengineering considered for each RCP scenario either brought radiative forcing back to P-I levels or to a particular forcing above P-I (the geoengineering forcing is labeled 'GEO' followed by the amount reduced; e.g. 'GEO 1.5' refers to an equivalent SRM geoengineering to bring anthropogenic forcing down by 1.5 W/m^2 by 2100). The SRM forcing was applied from 2020 with an e-folding time of 5 years and following the equivalent RCP scenario when available (i.e., 'RCP 6 & GEO 1.5' will have the same total forcing as 'RCP 4.5'). As for model training, the maximum and minimum monthly and weekly SST values were computed by adding observed present-day anomalies to UVic projected annual mean SST data (i.e. assuming variability remains unchanged). Future irradiance levels under SRM geoengineering were calculated by applying a -1 to -3% reduction to present observed values depending on emission scenario and desired total level of forcing. Additional variations in cloudiness patterns were not considered. All other environmental fields were kept at present values. Predictions were generated at 10-year intervals from 2010 to 2070 and for 1850 to establish the P-I baseline (for P-I projection map see Fig. S1.3, Appendix S1). The 2070 cut-off for future projections was chosen because 14% of coral reef cells are out of training range by this date under RCP 8.5. Bioclimatic Envelope Models become less reliable for forecasts that involve extrapolation to novel conditions because statistical relationships observed in training may no longer hold.

3. Results

Under the highest CO_2 scenario considered (RCP 8.5), year 2070 tropical SSTs are generally ~2-3°C higher than pre-industrial (P-I), with the strongest warming occurring in the western Pacific (Fig. 1a). Associated with rising atmospheric pCO_2 and invasion of fossil fuel CO_2 into the ocean, Ω_{Arag} falls by 1.5-2 units, with least change in upwelling areas (Fig. 1c). Under these conditions we forecast a marked decline in environmental suitability for shallow coral reef habitats across the central Indo-Pacific (Fig. 1e; see also Appendix S2). Elsewhere, conditions generally became less favorable, except for higher latitudes and upwelling regions. Values of a Habitat Suitability Index (defined as the mean probability of a coral reef being present, normalized as a percentage relative to P-I) fell from 93-97% in 2010, to 65-70% by 2070 (Fig. 2a & b). As an alternative way to measure impact on existing reefs, we also compared changes in suitability values across all 1° grid cells with present-day coral communities and reefs (i.e. with entries from the ReefBase v2000 database). These values declined substantially under all unmitigated RCP scenarios, and by 2070 had reached average values as low as 0.49 (RCP 8.5) compared to the P-I average of 0.62 for the BRT model output (Fig. 2c bottom row; MaxEnt values given in Fig. S2.7). The pattern of impact does not scale simply with increasing radiative forcing; instead an impact threshold is apparent at ~3 W/m^2. When levels of anthropogenic forcing were below 3 W/m^2 the probabilities on cells currently associated with reefs remained high (Figs. 2c and S2.7), and the area of significantly-reduced suitability was confined to within the central Indo-Pacific Warm Pool (IPWP; Fig. S2.1).

In the UVic simulations, application of SRM geoengineering sufficient to return the average global temperature to P-I levels leaves the tropics on average ~1°C cooler (Fig. 1b), similar to previous findings using fully coupled GCM models [e.g. *Lunt et al.*, 2008; *Irvine et al.*, 2010]. Because cooling increases CO_2 solubility, a subsidiary consequence of this SRM-driven over-cooling is that Ω_{Arag} is lower than under the unmitigated scenarios (Fig. 1d). The net result of cooler temperatures and further enhanced ocean acidification is that suitabilities for coral reefs (averaged across cells associated with modern reef sites) are lower under a geoengineering scenario of radiative forcing returned to 0 W/m^2 compared to P-I (i.e. 1:1 line in Fig. 2c for BRT results). In fact, suitabilities for a fully geoengineering climate are similar to those obtained for unmitigated RCP 4.5 and RCP 3 scenarios, although this reduction was less significant for MaxEnt (Fig. S2.7). In contrast, application of SRM geoengineering equivalent to reducing the forcing to 1.5 W/m^2 above P-I not only forestalls the projected decline in shallow-water reef habitat suitability across the central Indo-Pacific but leads to improved conditions in the central Pacific due to the residual warming there (Fig. 1f; Appendix S2). The probability histograms calculated for currently designated reef cells (Fig. 2c) show that all SRM geoengineering scenarios where forcing is reduced to 3 or 1.5 W/m^2 maintained reasonably favorable conditions and averages were preserved (0.56 to 0.62) near the P-I value (0.62).

4. Discussion and Conclusions

In our statistical models, unmitigated climate change leads to a SST-driven collapse in environmental suitability for shallow-water coral reefs, spreading from the center of the WPWP and across the central Indo-Pacific as radiative forcing increases beyond 3 W/m^2. For a radiative forcing of >4.5 W/m^2, the affected area encompasses the 'Coral Triangle', the richest region of biodiversity for corals and reef-associated fauna [e.g. *Tittensor et al.* 2010]. In contrast, declines in shallow water habitat suitable for coral reefs are averted in relatively aggressive SRM geoengineering scenarios in which net radiative forcing is restricted to 3 W/m^2 despite the existence of high pCO_2. Due to residual warming, forecast environmental conditions even improved slightly across the central Pacific; a region sparsely populated in terms of shallow coral reefs, but critical in terms of connectivity of reef-dependent species across the Pacific basin [e.g. *Lessios and Robertson, 2006; Mora et al., 2012*]. Similarly, upwelling regions were generally less impacted as a consequence of upwelled waters, previously isolated from the atmosphere, providing some buffering against acidification [Fig. 1c; *Lunt et al.*, 2008].

The difference in modeled response between unmitigated and geoengineered scenarios reflects the importance placed on SST variables; both MaxEnt and BRT use a combination of SST variables to explain 50-60% of the variation in models trained on present-day global shallow-water coral reef distribution [*Couce et al.,* 2012]. As a result, simulated future SST changes dominate predictions. Other environmental fields, in particular Ω_{Arag}, light availability and nutrients, are used to reinforce the SST-derived pattern and to model coral reef presence at regional scales where the correlation with temperature breaks down [*Couce et al.*, 2012]. Consequently, when global temperatures are controlled by SRM, the strongest negative responses map onto regions identified as sensitive during model development to reduced Ω_{Arag} and light availability: the Coral Triangle, south-west Pacific and South China Sea [*Couce et al.* 2012]. This spatial impact pattern was also observed in an empirically-supported modeling study on the response of global shallow-water coral reefs to future Ω_{Arag} reductions [*Silverman et al.* 2009].

The strongest decline in habitat suitability for shallow-water coral reefs corresponds to areas where maximum weekly SST increases above a threshold of 31.9°C, and is centered on the IPWP. Shallow-water coral reef ecosystems as a whole are very sensitive to elevated SSTs as evident from the recent observations of mass bleaching, mortality events and subsequent reef deterioration associated with SST anomalies [*Hoegh-Guldberg et al.* 2007]. However, the model focus on the IPWP as a thermally-sensitive region is supported by observations and empirical studies of physiological tolerances to thermal stress in reef-forming species of coral and coralline algae. Reduced thermal tolerance has been linked to both low SST variability environments [e.g. *Ateweberhan and McClanahan* 2010; *Teneva et al.* 2012] and synergistic stress from reduced Ω_{Arag} [e.g. *Anthony et al.* 2008]. The relative sensitivity of this region is further evident in recent observations of declining coral cover [*Bruno and Selig*, 2007] and exceptionally high susceptibility to mass bleaching events [*Donner et al.*, 2005; *Teneva et al.* 2012]. The amelioration of future SST warming is, therefore, of primary importance for minimizing impacts in this key region.

The relative dominance of SST in our statistical models helps explain why, in contrast to *Silverman et al.* [2009], our projections do not forecast a global collapse of coral reefs by ca. 560 ppm atmospheric CO_2. Instead, the potential presence of coral cover at high pCO_2 values (up to 677 ppm, by 2070 under RCP 8.5) is consistent with *Fabricius et al.* [2011] who observed massive *Porites* colonies growing within this range of geochemical conditions with no significant impact on calcification rates. Tropical coral reef ecosystems are treated as a single entity in our models, so our results should be considered a simplified first order approximation and cannot be directly compared to the substantial changes in coral community composition and diversity vs. environmental gradient observations also observed by *Fabricius et al.* [2011]. The future loss of biodiversity is likely to be significant under high pCO_2, but the models can not separate potentially significant shifts in the distributions of individual reef-forming species and so the modeled habitat suitability response is likely muted. Future use of correlative models created at the species (of functional type) level may provide a means to start addressing this question.

To what degree can the statistical model projections be treated as robust in the face of potential future changes in both variable correlation and spatial patterns? Under SRM scenarios, the first order inverse correlation that exists between SST variables and Ω_{Arag} in the modern surface ocean no longer holds. As a result, the two Bioclimatic Envelope Model class types used in our study might have yielded divergent projections, because of their different internal use of correlated variables [*Couce et al.*, 2012; Appendix S1]. Instead, the strong agreement between the MaxEnt and BRT predictions (Appendix S2) suggests the models are not over-relying on present-day correlations between variables, thus increasing confidence in the projections. There is also an implicit decoupling between specific local and/or hourly conditions occurring at a reef site and the relatively large spatial (1° x 1° scale) and weekly-to-annual average data employed in our models. However, as long as local reef environments change in tandem with large-scale 'open ocean' changes, our results should not be substantially biased.

It is important to note that it becomes necessary to extrapolate when variables exceed the range of present-day environmental values used for model calibration (e.g. when mean annual SST increases over 31.4°C). Both BRT and MaxEnt techniques deal with such situations by setting the response outside of training range at the level set for the nearest most extreme within-training value. A detailed discussion of the effect of the chosen extrapolation method on the results is given in Appendix S3. The net result is a constant positive response in the case of increasing Ω_{Arag} (e.g. experienced under P-I conditions) and a conservative assessment of the negative impacts of warming by setting a constant negative response in the case of higher SSTs. Grid cells with novel conditions for which the extrapolation method strongly impacts predictions are explicitly shown in the results (hatched areas in Figs. 1e and 1f and in the histograms in Figs. 2c and S2.7). By 2070 these areas of problematic extrapolation affect a minority of cells where shallow-water coral communities and reefs are currently found (0-14%; on average 2.5%), and conclusions remain unaltered by excluding these areas (e.g. the general reduction in shallow reef habitat suitability under all unmitigated RCP scenarios in Figs. 2c and S2.7 is a robust finding). In fact, the extrapolation of a negative response onto extreme SSTs imposed by both models would be a logical decision from empirically-driven evidence [e.g. thermal damage limits of coral reviewed in *Brown and Cossins* 2011]. Significantly, this response implies that the dataset used to calibrate our statistical models contains sites where present-day shallow-water coral reef distribution is already limited by thermal thresholds. The dataset does not, however, include coral reefs from the Red Sea and Arabian Gulf, which tolerate similar extreme maximum SSTs but are potentially conditioned by very high SST variability [*Ateweberhan and McClanahan* 2010], because it was not possible to simulate conditions using the UVic model in these enclosed seas. While assessment of habitat beyond 2070, and under CO_2 concentrations higher than the maximum we consider here (677 ppm at year 2070 under RCP8.5), may be desirable for a fuller and longer-term picture, the utility of the Bioclimatic Envelope Modeling approach becomes increasing limited as more of the ocean exceeds training limits.

Overall, our work highlights the complex patterns of global change induced by even simple (and spatially uniform) geoengineering scenarios, with consequences that can be non-obvious. Specifically, we find that tropical over-cooling by full geoengineering, together with a relatively low comparative sensitivity to Ω_{Arag} in our models, creates an apparent 'optimum' for shallow coral reef habitat (this is particularly evident in the BRT model output; Figs. 2a, 2c, and S2.8). This optimum occurs under environmental conditions corresponding to a partially, but not fully, mitigated high CO_2 climate (i.e. SRM geoengineering of radiative forcing to 1.5 W/m^2 above P-I). A high degree of geoengineering with a global net residual warming acts to even out surface meridional temperature gradients while preventing tropical over-cooling, to the net advantage of tropical corals. This outcome is possibly exaggerated because terrestrial carbon storage feedback cannot be explicitly accounted for under the fixed atmospheric CO_2 concentrations of the RCP-based approach. For example, Matthews *et al.* [2009] found that SRM could slightly mitigate ocean acidification, although Ω_{Arag} would still decrease, due to a simulated increase in terrestrial CO_2 uptake and hence atmospheric pCO_2 drawdown.

In conclusion, while SRM geoengineering fails to tackle the causes or consequences of ocean acidification, the detrimental effect of higher SSTs appears to strongly out-weigh the impacts of reduced Ω_{Arag} for tropical shallow-water coral reefs when treated as a single entity. Further studies are needed to resolve potential changes in coral reef community composition and biodiversity, however, severe reductions in the area of suitable shallow-water coral reef habitat might be averted if anthropogenic forcing is limited $\leq$3 W/m^2 or returned below this level via SRM. Overall, our work highlights the need for a multi-stressor and spatially-explicit framework in assessing ecological implications of future global change, whether mitigated or not, so that the complex patterns of induced change and the non-linear combinations of environmental pressures can be adequately evaluated.

5. Acknowledgements

This work was supported by a U. Bristol postgraduate scholarship to E.C., a UK NERC postgraduate studentship to P.J.I., a Royal Society Advanced Fellowship to A.R., and a RCUK Academic Fellowship to E.J.H. L.J.G. was funded by the UK Ocean Acidification Research Program (NE/H017453/1) and EPSRC grant EP/I014721/1. We thank H. Russell and A. Wilmot-Sitwell for additional funding to support E.C.

6. References

Angel, R. (2006), Feasibility of cooling the Earth with a cloud of small spacecraft near the inner Lagrange point (L1), *Proc. Natl. Acad. Sci. U. S. A.*, *103*(46), 17184-17189, doi: 10.1073/pnas.0608163103.

Anthony, K. R. N., D. I. Kline, G. Diaz-Pulido, S. Dove, and O. Hoegh-Guldberg (2008), Ocean acidification causes bleaching and productivity loss in coral reef builders, *Proc. Natl. Acad. Sci. U. S. A.*, *105*(45), 17442–17446, doi: 10.1073/pnas.0804478105.

Ateweberhan M., and T.R. McClanahan (2010), Relationship between historical sea-surface temperature variability and climate change-induced coral mortality in the western Indian Ocean, *Mar. Pollut. Bull.* 60, 964–970.

Brown, B.E., and A.R. Cossins (2011), The potential for temperature acclimatisation of reef corals in the face of climate change, in: *Coral Reefs: an Ecosystem in Transition* edited by Z. Dubinsky and N. Stambler, pp. 421–433, Springer Dordrecht.

Bruno, J.F., and E.R. Selig (2007), Regional decline of coral cover in the Indo-Pacific: timing, extent, and subregional comparisons, *PLoS ONE*, 2, e711, doi:10.1371/journal.pone.0000711.

Couce, E., A. Ridgwell, and E. J. Hendy (2012), Environmental controls on the global distribution of shallow-water coral reefs, *Journal of Biogeography*, 39(8), 1508-1523, doi: 10.1111/j.1365-2699.2012.02706.x.

Crutzen, P. J. (2006), Albedo enhancement by stratospheric sulfur injections: A contribution to resolve a policy dilemma?, *Clim. Change*, *77*(3-4), 211-219, doi: 10.1007/s10584-006-9101-y.

Donner, S. D., W. J. Skirving, C. M. Little, M. Oppenheimer, and O. Hoegh-Guldberg (2005), Global assessment of coral bleaching and required rates of adaptation under climate change, *Global Change Biol.*, *11*(12), 2251-2265. doi: 10.1111/j.1365-2486.2005.01073.x.

Fabricius, K. E., C. Langdon, S. Uthicke, C. Humphrey, S. Noonan, G. De'ath, R. Okazaki, N. Muehllehner, M. S. Glas, and J. M. Lough (2011), Losers and winners in coral reefs acclimatized to elevated carbon dioxide concentrations, *Nature Clim. Change*, *1*(3), 165-169.

Friedman, J. H. (2001), Greedy function approximation: A gradient boosting machine, *Ann. Stat.*, *29*(5), 1189-1232.

Hoegh-Guldberg, O. et al. (2007), Coral reefs under rapid climate change and ocean acidification, *Science, 318* (5857), 1737-1742, doi: 10.1126/science.1152509.

Hönisch, B., et al. (2012), The Geological Record of Ocean Acidification, *Science, 335*(6072), 1058-1063.

Irvine, P. J., A. Ridgwell, and D. J. Lunt (2011), Climatic effects of surface albedo geoengineering, *J. Geophys. Res.*, *116*, D24112, doi:10.1029/2011JD016281.

Kleypas, J. A., R. W. Buddemeier, D. Archer, J. P. Gattuso, C. Langdon, and B. N. Opdyke (1999), Geochemical consequences of increased atmospheric carbon dioxide on coral reefs, *Science*, *284* (5411), 118-120, doi: 10.1126/science.284.5411.118.

Latham, J., and M. H. Smith (1990), Effect on Global Warming of Wind-Dependent Aerosol Generation at the Ocean Surface, *Nature*, 347 (6291), 372-373, doi:10.1038/347372a0.

Lessios, H. A., and D. R. Robertson (2006), Crossing the impassable: genetic connections in 20 reef fishes across the eastern Pacific barrier, *Proc. R. Soc. B., 273* (1598), 2201-8*,* doi:10.1098/rspb.2006.3543.

Lunt, D. J., A. Ridgwell, P. J. Valdes, and A. Seale (2008), "Sunshade World": A fully coupled GCM evaluation of the climatic impacts of geoengineering, *Geophys Res Lett*, *35*(12), L12710, doi:10.1029/2008GL033674.

Matthews, H. D., L. Cao, and K. Caldeira (2009), Sensitivity of ocean acidification to geoengineered climate stabilization, *Geophys Res Lett*, *36*, L10706, doi:10.1029/2009GL037488.

Mora, C., E. A. Treml, J. Roberts, K. Crosby, D. Roy, and D. P. Tittensor (2012), High connectivity among habitats precludes the relationship between dispersal and range size in tropical reef fishes, *Ecography*, *35*(1), 89-96.

Moss, R. H., et al. (2010), The next generation of scenarios for climate change research and assessment, *Nature*, *463*(7282), 747-756, doi:10.1038/nature08823.

Phillips, S. J., R. P. Anderson, and R. E. Schapire (2006), Maximum entropy modeling of species geographic distributions, *Ecol. Modell.*, *190*(3-4), 231-259, doi:10.1016/j.ecolmodel.2005.03.026.

ReefBase (2000), ReefBase 2000: improving policies for sustainable management of coral reefs, in *CD-ROM*, edited, International Centre for Living Aquatic Resources Management, Philippines.

Schmittner, A., A. Oschlies, H. D. Matthews, and E. D. Galbraith (2008), Future changes in climate, ocean circulation, ecosystems, and biogeochemical cycling simulated for a business-as-usual CO_2 emission scenario until year 4000 AD, *Global Biogeochem. Cycles*, *22*(1), GB1013, doi:10.1029/2007GB002953.

Silverman, J., B. Lazar, L. Cao, K. Caldeira, and J. Erez (2009) Coral reefs may start dissolving when atmospheric CO_2 doubles. *Geophys Res Lett*, *36*, L05606, doi:10.1029/2008GL036282.

Teneva, L., M. Karnauskas, C.A. Logan, L. Bianucci, J.C. Currie, and Kleypas, J.A (2012) Predicting coral bleaching hotspots: The role of regional variability in thermal stress and potential adaptation rates. *Coral Reefs*, *31* (1), 1-12, doi: 10.1007/s00338-011-0812-9.

Thuiller, W., S. Lavorel, M. B. Araújo, M. T. Sykes, and I. C. Prentice (2005), Climate change threats to plant diversity in Europe, *Proc. Natl. Acad. Sci. U. S. A. 102*, 8245-8250, doi: 10.1073/pnas.0409902102

Tittensor, D. P., et al. (2010), Global patterns and predictors of marine biodiversity across taxa, Nature, 466, 1098-1011, doi:10.1038/nature09329.

Turley, C., M. Eby, A. J. Ridgwell, D. N. Schmidt, H. S. Findlay, C. Brownlee, U. Riebesell, V. J. Fabry, R. A. Feely, and J. P. Gattuso (2010), The societal challenge of ocean acidification, *Mar. Pollut. Bull.*, *60*(6), 787-792., doi: 10.1016/j.marpolbul.2010.05.006.

Weaver, A. J., et al. (2001), The UVic Earth System Climate Model: Model description, climatology, and applications to past, present and future climates, *Atmos.–Ocean*, *39*(4), 361-428.

Figure captions

Figure 1: Simulated spatial anomalies, year 2070 minus pre-industrial (P-I), of sea surface temperature (SST; top a, b) and aragonite saturation state (Ω_{Arag}; bottom c, d) under RCP 8.5 (a, c) and with SRM geoengineering returning total anthropogenic radiative forcing to P-I values in the 'RCP 8.5 & GEO 8.5' scenario (b, d). Change in shallow-water tropical coral reef habitat suitability between 2070 and P-I, averaged from BRT and MaxEnt model outputs for RCP 8.5 (e) and 'RCP 8.5 & GEO 7', with SRM geoengineering to reduce anthropogenic radiative forcing to 1.5 W/m^2 above P-I by 2100 (f). Green dotted line corresponds to 0 change; black hatched pattern overlays area where projections move beyond training range with significant influence on predictions. For other scenarios see Appendix S2.

Figure 2: Habitat Suitability Index (defined as the average suitability for coral reefs within the shallow-water mask between 60°S to 60°N) for BRT (a) and MaxEnt (b). Values are normalised to pre-industrial (P-I) predictions and show the evolution at 10-year intervals until 2070 under the unmitigated RCP 8.5 scenario (black) and various level of SRM (lighter colours show progressively higher degrees of SRM intervention). For all other scenarios see Appendix S2, Figs. S2.8 and S2.9. Histograms showing the percentage of reef cells within each BRT modelled suitability value (c). The bottom-left histogram is for P-I conditions; all remaining histograms are for 2070 conditions and reflect potential changes in suitability under the four unmitigated RCPs (bottom row, along x-axis) and various levels of SRM geoengineering (y-axis). Reef cells are cells

where reefs or non-reef coral communities are presently found [ReefBase v2000]. Novel environmental conditions, compared to the 1990 values used for model training, are simulated by UVic Earth System Climate Model for SST and Ω_{Arag} on some reef cells. The solid coloured histogram bars contain all cells either with environmental conditions within the bioclimatic envelope used to train the models or where out-of-range variables do not significantly affect predictions. The average suitability value ($\bar{x}$) of reef cells for each scenario is calculated from this sample set. Cells where predictions are less reliable (i.e. SST and/or Ω_{Arag} values out of training range and MaxEnt clamping value > 0.1; see Appendix S3) are indicated by hatched pattern and have been excluded from the calculated average.

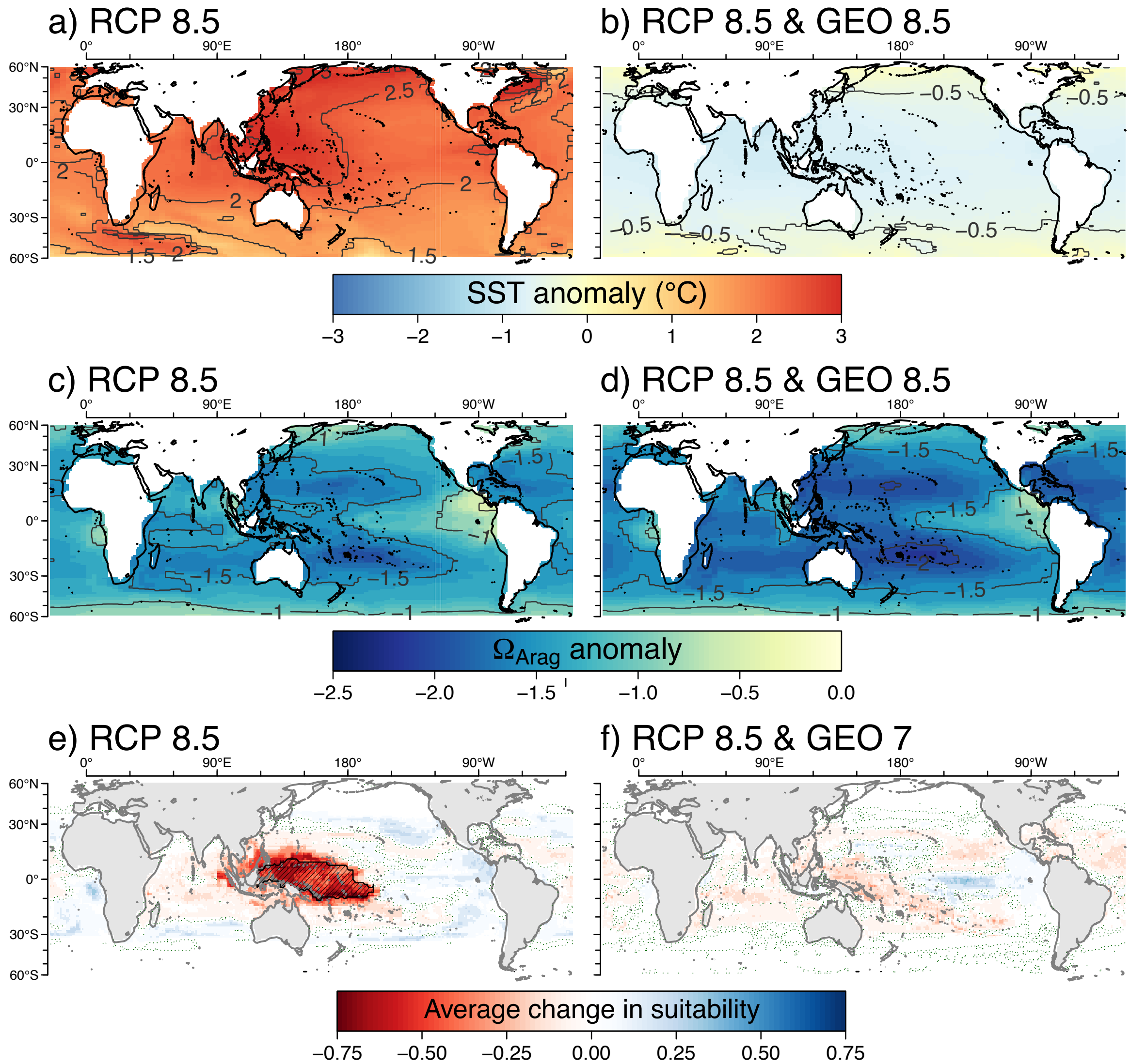
a) RCP 8.5
b) RCP 8.5 & GEO 8.5
SST anomaly (°C)
–3 –2 –1 0 1 2 3
c) RCP 8.5
d) RCP 8.5 & GEO 8.5
Ω_Arag anomaly
–2.5 –2.0 –1.5 –1.0 –0.5 0.0
e) RCP 8.5
f) RCP 8.5 & GEO 7
Average change in suitability
–0.75 –0.50 –0.25 0.00 0.25 0.50 0.75
0° 90°E 180° 90°W
60°N 30°N 0° 30°S 60°S

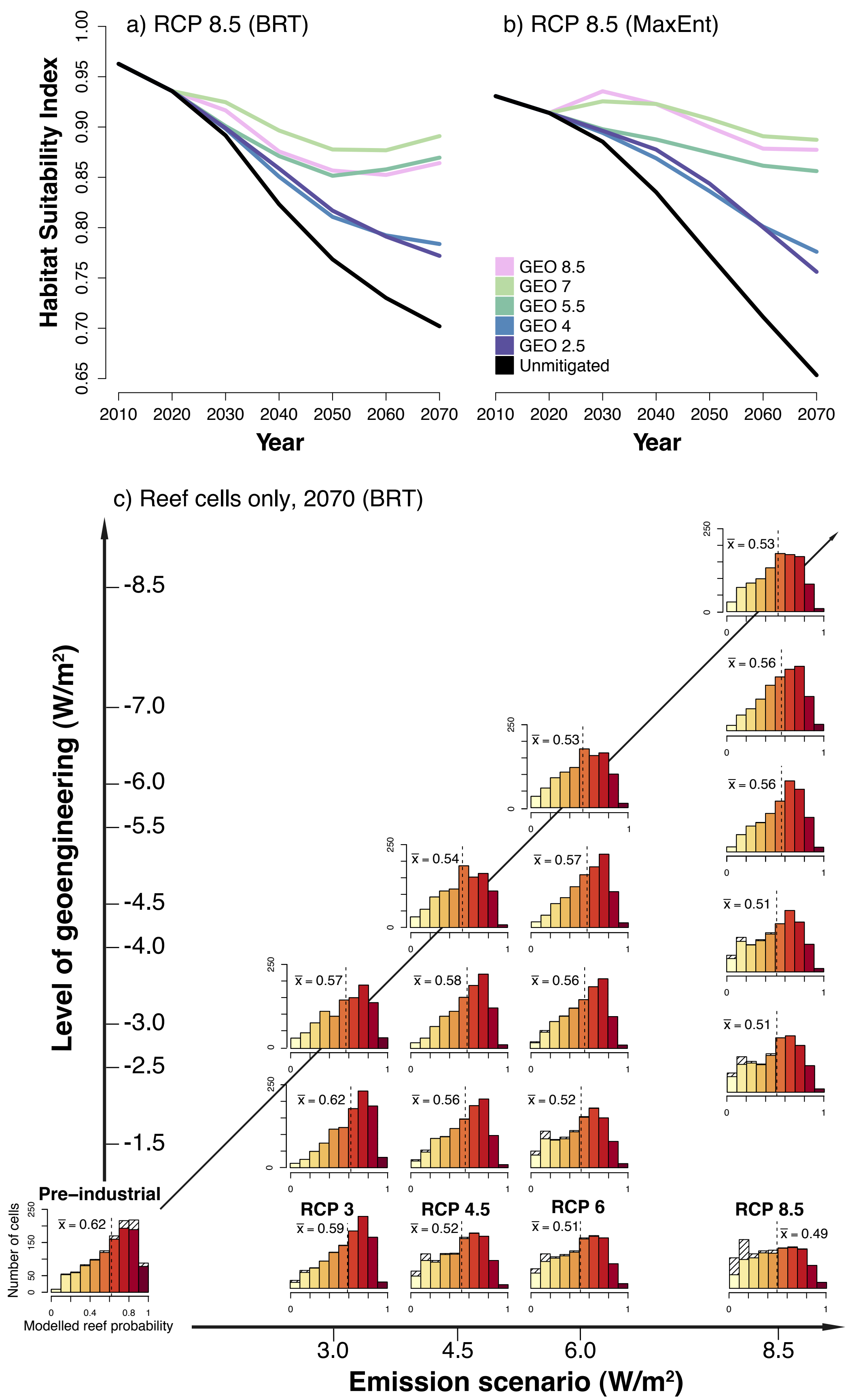
a) RCP 8.5 (BRT)
b) RCP 8.5 (MaxEnt)
Habitat Suitability Index
Year
GEO 8.5
GEO 7
GEO 5.5
GEO 4
GEO 2.5
Unmitigated
c) Reef cells only, 2070 (BRT)
Level of geoengineering (W/m²)
Pre–industrial
Number of cells
Modelled reef probability
RCP 3
RCP 4.5
RCP 6
RCP 8.5
Emission scenario (W/m²)